Plant Prod. Sci. 15(4): 293—309 (2012)

Estimating Rice Leaf Greenness (SPAD) Using Fixed-Point Continuous Observations of Visible Red and Near Infrared Narrow-Band Digital Images

Michio Shibayama[1], Toshihiro Sakamoto[1], Eiji Takada[2], Akihiro Inoue[2], Kazuhiro Morita[3], Takuya Yamaguchi[3], Wataru Takahashi[3] and Akihiko Kimura[4]

([1]National Institute for Agro-Environmental Sciences, 3-1-3 Kannondai, Tsukuba, Ibaraki 305-8604, Japan;
[2]Toyama National College of Technology, 13 Hongo-machi, Toyama, Toyama 939-8630, Japan;
[3]Toyama Prefectural Agricultural, Forestry and Fisheries Research Center, 1124-1 Yoshioka, Toyama, Toyama 939-8153, Japan;
[4]Kimura OyoKogei Inc., 292-4 Takagi, Saitama, Saitama 331-0071, Japan.)

Abstract: A narrow-band dual camera system demonstrated a new close-range sensing technique to seasonally track trends in leaf greenness in rice paddies. A weatherproof digital imaging system for the visible red (RED, 620–650 nm) and near infrared band (NIR, 820–900 nm) was positioned 12 m above a 600-m^2 rice field. During the 2009 and 2010 paddy rice seasons, the system automatically logged images at 10-min intervals throughout the day. Radiometric corrections for the images utilized solar irradiance sensors and prior calibration to calculate 0900-1500 JST daily-averaged reflectance factors (DARF). The DARF in RED (DARF-RED) and NIR (DARF-NIR) values were transformed to provide a daily-averaged normalized difference vegetation index (DA-NDVI). The DA-NDVI increased more rapidly in the vegetative growth period, and reached an asymptotic plateau earlier than the DARF-NIR. From transplanting to harvest, leaf greenness values (measured by the SPAD index) were measured for the central part of the uppermost leaves of targeted canopies weekly with a chlorophyll meter. We developed a leaf greenness index (LGI), the ratio of DA-NDVI to DARF-NIR, and a simple calculation method for area means to reduce the background effect. The modified area means of LGI followed the seasonal trend in SPAD value well; its pattern was inherently different from the patterns of any of the original three parameters: DARF-RED, DARF-NIR or DA-NDVI. Throughout the paddy seasons in the two years, a regression equation for estimating SPAD values using the LGI, daily solar radiation, the cosine of angle between the view and the meridian directions and the cosine of culmination solar zenith angle performed favorably ($R^2 = 0.815$). The nitrogen concentration per dry plant hill (g kg^{-1}) had a close relation to the SPAD values estimated using the equation.

Key words: Digital camera, NDVI, Nitrogen, Reflectance factor, Rice, SPAD.

One of the essential factors of carbon assimilation per unit land area after heading is the rate of carbon assimilation per unit leaf area, and an effective cultural practice for increasing it is to topdress at the late spikelet initiation stage and at the full heading stage (Matsushima, 1976). Technically, the nutrient condition of crop plants at critical stages should be estimated in situ to determine the appropriate amount of topdressing. Nitrogen concentration (g kg^{-1}, dry weight basis) of the leaf or whole plant has already proven to be relevant to many requirements of crop monitoring to assess the nutrient condition of rice plants. It has been used to determine the appropriate timing of application and amount of topdressing nitrogen fertilizer for normal growth and development of the crop during vegetative growth (Wada, 1969; Balasubramanian, 1999; Dobermann, 2003) and for preharvest assessment of

Received 6 December 2011. Accepted 19 February 2012. Corresponding author: M. Shibayama (shibayama@agri.kagoshima-u.ac.jp, fax +81-99-285-8525, Present adress; Faculty of Agriculture, Kagoshima University, 1-21-24 Korimoto, Kagoshima 890-0065, Japan). This work was financially supported by Grant-in-Aid for Science Research (C) (No. 21580320) from the Ministry of Education, Culture, Sports, Science and Technology of Japan and the Japan Society for the Promotion of Science.

Abbreviations: DA-NDVI, daily-averaged normalized difference vegetation index; DARF, daily-averaged reflectance factor; DS, duration of sunshine; LAI, leaf area index; LGI, leaf greenness index; NIR, near infrared; PAR, photosynthetically active radiation; PDC, portable dual-band digital camera; RF, reflectance factor; SR, daily solar radiation; SZ, solar zenith angle.

the yield and grain quality in the maturing period (Abe et al., 2007; Mori et al., 2010). Nitrogen content variation among plant hills and locations in the plot or field are important for precision farming (Ahmad et al., 1999). Optimal nitrogen application is also imperative for both efficient and sustainable farming (Spiertz, 2010).

Due to the high cost of determination of nitrogen concentration by destructive chemical techniques, nondestructive techniques for the determination of nitrogen concentration have been developed, such as the leaf color plate or chart (Matsushima et al., 1970; Takebe and Yoneyama, 1989; Sen et al., 2011), the hand-held optical chlorophyll meter (Takebe and Yoneyama, 1989; Suenobu et al., 1994; Turner and Jund, 1994; Esfahani et al., 2008; Huang et al.,2008; Lin et al., 2010), and spectral reflectance measurement by ground-based (Shibayama and Akiyama, 1986b; Takebe et al., 1990; Takahashi et al., 2000; Zhu et al., 2007) or air- and space-borne remote observation (Haboudane et al., 2002; Asaka and Shiga, 2003; Asaka et al., 2006; Tanaka, et al., 2008). In these techniques, the leaf color or spectral reflectance is related to the content (per unit leaf area) or density (per unit land area) of the photosynthetic pigments chlorophyll a and chlorophyll b, and assume a close relationship between the content of leaf chlorophyll and nitrogen concentration (Peng et al., 1995; Lee et al., 2011).

Each technique has strengths and limitations. The economical leaf color chart technique depends on the user's ability and experience as well as weather conditions. The widely used chlorophyll meter does not require skill or natural illumination but still requires repeated contiguous sample measurements in the field, which requires considerable time and labor when the targeted crop has a certain variation in chlorophyll content among plants and/or leaves and size in space. In particular, measurements in waterlogged paddies are formidable. On the other hand, field reflectance measurement generally requires costly equipment, such as a spectroradiometer, and fair and stable weather conditions, so the reliability or reproducibility of the data is sometimes problematic. Adverse weather during the cropping season frequently disturbs collection of full and timely optical remote sensing data from airplanes and satellites (Akiyama and Kawamura, 2003). Direct reflection of sunlight from leaves may cause problems under sunny and windy conditions because the unified-view sensor of a radiometer cannot separate abnormal targets from correct ones (Takebe et al., 1990).

Imagery observation may solve the above problem, several papers have described advantages of video or digital cameras in applications for leaf color assessment (e.g., Nakatani and Kawashima, 1994; Kawashima and Nakatani, 1998; Jia et al., 2004; Ku et al., 2004; Casadesus et al., 2007; Takemine et al., 2007). The advantages of image data taken for a certain area in a short time prevail over the other methods. Hand-held digital cameras sensitive to both visible and near infrared wavelengths are available for agricultural and vegetation studies (White et al., 2000; Omine, 2007; Okada and Ikeba, 2008; Sakamoto et al., 2010). Imaging spectrometers with higher spectral resolution, may be effective for basic studies, but available imagers are too costly and unwieldy for practical field work (Inoue and Peñuelas, 2001; Minekawa et al., 2007; Shibayama et al., 2009a).

For paddy rice leaf color and nitrogen concentration assessments, advanced research has supported the possibility of using commercial color digital cameras (Matsuda et al., 2003; Nagano and Shigedomi, 2005). Of course, changing weather conditions affecting measurement times and the viewing and illumination geometry of camera images have been major obstacles. Most studies have introduced a reference panel or color chart to correct varying illumination and camera sensitivity (Okada and Ikeba, 2008). Validation is also necessary for varietal, year-to-year and seasonal responses of indices derived from the images. In particular, the indices should move with seasonal changes in nitrogen content or leaf color to monitor the crop's nutrient status at specific critical times of earlier growth stages. In other words, the indices developed need to correctly follow the seasonal changes of chlorophyll content or leaf color.

For measuring fractional cover and leaf area index (LAI) in shrublands, White et al. (2000) suggested that long-term monitoring would be optimized by mounting a multiband digital camera on a tower platform. Few practical applications have been done from that viewpoint. In addition, assessment of crop chlorophyll status from remotely sensed data requires indices that are both responsive to chlorophyll concentration and insensitive to background and LAI effects (Daughtry et al., 2000). Chlorophyll density per unit land area should be easier to estimate than leaf chlorophyll concentration by field radiometric measurement (Shibayama and Akiyama, 1986a). On the contrary, optical remote detection of chlorophyll content would be a more challenging task than chlorophyll density. However, Haboudane et al. (2002) developed a predictive index for corn leaf chlorophyll content for LAI values varying from 0.5 to 6 from above-canopy reflectance data.

The techniques for collecting fixed-point, seasonally continuous observations of visible red and near infrared band reflectance images of paddy rice canopies and applications for rice nitrogen uptake and LAI predictions have been described (Shibayama et al., 2009b, 2011a, 2011b). These agronomic variables are measured on a unit land area basis. However, leaf color, which is related to chlorophyll content, and nitrogen concentration of the plant are also essential for practical farming management. Using the two-band digital camera imagery, Takada et al.

Table 1. Summary of cultivation conditions in experimental rice paddy plots.

Year of experiment	Variety of paddy rice	Fertilization (g N m^{-2})	Trans-planting date	Heading time
2009	Koshihikari Nipponbare	Basal fertilization: 4 Topdressing: 1 or 3 (=2+1)†	28 May	9 August (Koshihikari) 18 August (Nipponbare)
2010	Koshihikari Nipponbare	Basal fertilization: 4 Topdressing: 0, 1 or 3 (=2+1)†	31 May	5 August (Koshihikari) 16 August (Nipponbare)

† Split applications at the late spikelet initiation and at the full heading stages measured for 'Koshihikari'.

(2009) showed a possibility for monitoring seasonal changes in the product of rice leaf SPAD value and number of stems, which was roughly a plant hill-oriented parameter. However, not many quantitative studies have been done to establish whether two-band digital camera imagery could have comparable performance to seasonal detection of changes in rice leaf chlorophyll content.

We carried out a biennial study on the fixed-point continuous two-band imaging technique to make stable predictions of seasonal changes in rice leaf color measured by the SPAD value. Two of Japan's major rice varieties, early and medium maturing varieties, were planted in two cropping seasons, and the nitrogen concentration of sample plant hills was periodically measured in the first-year experiment. From the standpoint of pursuing accuracy in chlorophyll content prediction, direct chemical measurements of leaf samples to estimate chlorophyll content are preferable to merely using SPAD. However, we did not convert from SPAD values to chlorophyll or nitrogen content because SPAD values have been used widely for crop monitoring without conversion when crop species and varieties are limited (Johnkutty and Palaniappan, 1996). This labor-saving approach increased the number of observations obtained under a given amount of research resources. Our objectives were to elaborate a methodology to replace rice leaf SPAD measurement using a digital imaging technique and to validate the year-to-year applicability of the methodology in field experiments.

Materials and Methods

1. Instruments

The specifications of the portable dual-band digital camera (PDC; Kimura OyoKogei Inc., Saitama, Japan) used to make measurements in 2009 and 2010 were as described by Shibayama et al. (2009b). Two digital camera boards, one for visible red (RED, 630–670 nm) and another for near infrared (NIR, 820–900 nm) were installed in a waterproof housing. The PDC was mounted on a remotely controlled motorized camera platform that adjusted the view zenith angle of the PDC on top of a 12-m-high pole.

We used the term reflectance factor (RF) for observed radiometric value instead of reflectance. The whole incident and reflected radiant flux (W) values on the target from all directions are needed to measure reflectance, whereas RF indicates the intensity of light reflected from the target divided by that reflected from a perfectly reflecting diffuser illuminated under the same lighting conditions, view directions and view solid angles (Emori and Yasuda, 1985). The configuration of the PDC results in observations that are closer to the RF measurement than reflectance. The PDC was adjusted for radiometric values prior to field measurements in 2008 and estimated RF values were validated by placing a gray-scale board at the center of the viewed field (Shibayama et al., 2011a). The PDC has separate solar irradiance sensors fitted with the same-spec filters used in the cameras; the measured solar irradiance provides a correction for fluctuating illumination to enable calculation of the instantaneous values of the RF of each band.

2. Sample site and agronomic survey

The experimental paddy field was located on the campus of the National Institute for Agro-Environmental Sciences in Tsukuba, Japan (36º 01′ 27″ N 140º 06′ 27″ E, 25 m a.s.l.). Table 1 summarizes the cultivation conditions of the test rice plants grown in 2009 and 2010. In both years, plots of rice (*Oryza sativa* L. ssp. *japonica*, var. 'Koshihikari' and 'Nipponbare') were established in two adjacent concrete-framed paddy fields of 10 m×50 m filled with alluvial soil. Seedlings of both varieties were transplanted on 28 May 2009 and 31 May 2010, using a ride-on transplanter in approximately northeast-southwest rows with a row width of 30 cm and an inter-hill space of 15 cm. The experimental field is equipped with an irrigation system with a water valve for each fertilization plot. The plots were separated with a plastic corrugated strip-shaped sheet, and flooded irrigation was employed except during midseason drainage.

Common basal nitrogen 4 g N m^{-2} was applied with N-P-K compound fertilizer for whole plots, with split dressing only for high-nitrogen level plots (H) at the late spikelet initiation stage (2 g N m^{-2}) and at the full heading stage (1 g N m^{-2}). Low (L) nitrogen plots received no topdressing and medium (M) nitrogen level plots received topdressing of 1 g N m^{-2} only at the late spikelet initiation stage. The nitrogen was also topdressed by the N-P-K compound fertilizer. The variety 'Koshihikari' matures earlier than 'Nipponbare' in the test location. To simplify

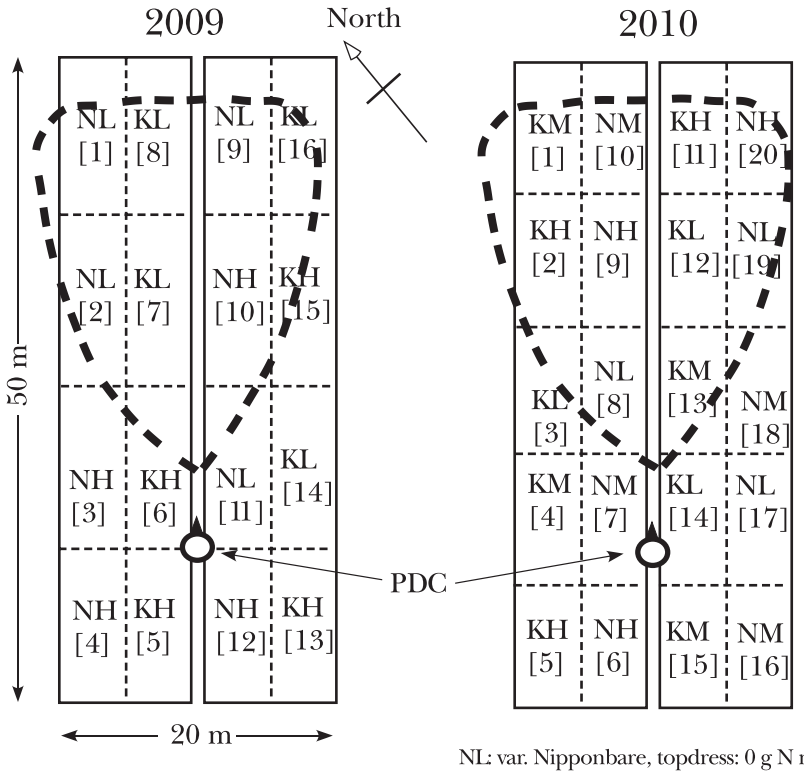

NL: var. Nipponbare, topdress: 1 g N m^{-2}

NH: var. Nipponbare, topdress: 3 g N m^{-2}

KL: var. Koshihikari, topdress: 1 g N m^{-2}

KH: var. Koshihikari, topdress: 3 g N m^{-2}

NL: var. Nipponbare, topdress: 0 g N m^{-2}

NM: var. Nipponbare, topdress: 1 g N m^{-2}

NH: var. Nipponbare, topdress: 3 g N m^{-2}

KL: var. Koshihikari, topdress: 0 g N m^{-2}

KM: var. Koshihikari, topdress: 1 g N m^{-2}

KH: var. Koshihikari, topdress: 3g N m^{-2}

Fig. 1. Top-view schemata of the trials for a rice paddy field in 2009 (left) and 2010 (right). A portable dual-band digital camera (PDC) was fixed on top of a 12-m-high pole; the dashed lines indicate the approximate viewing fields. The numbers 1 through 16 and 20 in square brackets represent the plot identifiers.

treatment, the growth stages were measured only for 'Koshihikari', and the topdressings were applied on same dates for both varieties. The 2009 and 2010 experimental designs are illustrated in Fig. 1.

The SPAD values were measured in each plot using a SPAD-502 chlorophyll meter (Konica Minolta Inc., Tokyo, Japan) from 18 June to 18 September 2009 at about 7-day intervals. In 2010, we measured from 18 June to 10 September at about 7-day intervals using a newer model, the SPAD-502plus. The uppermost expanded leaves on five consecutive plant hills were measured and the five values were immediately averaged. The optical sensing component was clipped to the central part of the measured leaf, avoiding the midrib. Three groups of five hills were chosen in each plot. The arithmetic mean and standard deviation of the three values were used for further analysis. The measured plants were not strictly fixed, but approximately similar plant-hill groups were targeted at each time of measurement.

The biennial study is based on the assumption that SPAD values measured with hand-held optical sensors (SPAD-502 and -502plus) are reliable and compatible. We tested the relationship between the measured values from the old model (SPAD-502) and the new model (SPAD-502plus) for the same rice leaf blades. The tests were repeated on three dates: 18 June and 2 and 23 July 2010. A simple regression from the new to old SPAD values indicated that the change in intercept value was not significant (≈ 0), the slope was 0.97 (at the 5% confidence interval: 0.90–1.05) and the R^2 value was 0.93 for 50 observations. We considered that the relationship was close to 1:1, so SPAD values from the two sensors could be used without interconversion in this work.

In 2009, three plant hills each were sampled from the 16 plots on 25 June, 9 and 23 July, 6 and 20 August and 3 September, and the aboveground plant parts were oven-dried at 70°C. We requested quantitative determination of plant nitrogen content (g N kg^{-1}) to a private chemical analysis firm (Environmental Research Center, Tsukuba, Ibaraki, Japan). The plant materials were ball-milled and the total nitrogen content was measured by the dry combustion method.

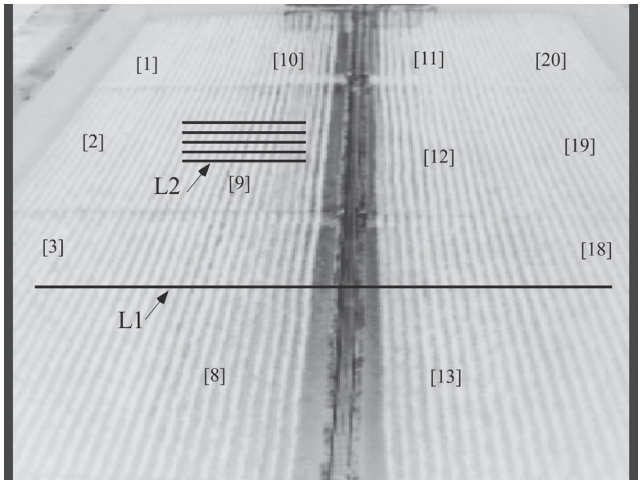

Fig. 2. Daily-averaged NDVI (DA-NDVI) image observed for paddy rice plots on 26 June, 2010. L1 indicates the cross-sectional line for sampling the exemplary values shown in Fig. 4. L2 indicates five sample lines for extracting radiometric values from each plot in daily-averaged images. The numbers in square brackets represent the plot identifiers.

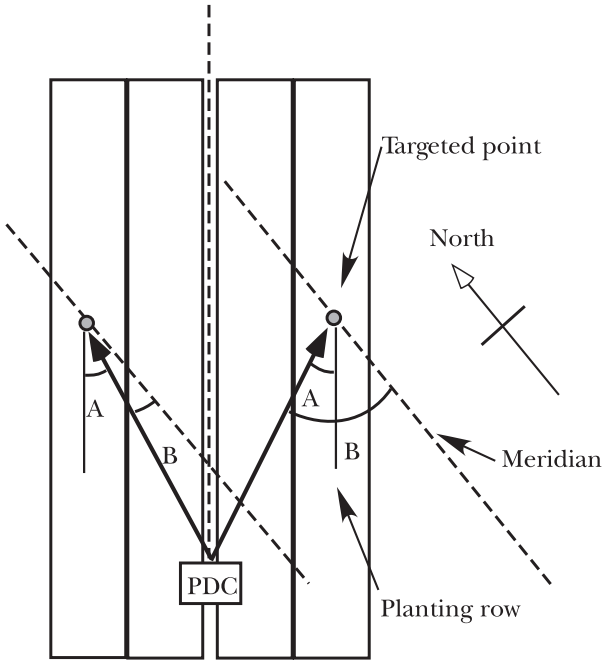

Fig. 3. Definitions of view angles A and B used in the study.

3. Image collection

The PDC system was set up on 1 June 2009, 4 days after transplanting, and 31 May 2010, right after transplanting. Images were recorded at 10-min intervals from 0700 to 1700 JST daily until 9 October 2009, and until 15 September 2010 at five arbitrary exposure speeds for both bands. The PDC view azimuth direction was from southwest to northeast and the view zenith angle was approximately 56º.

The PDC digital number ranged between 0 and 255 (8 bits) and the images measured 640×480 pixels. Each digital number in the image was spatially corrected using equations provided for each band and exposure speed (Shibayama et al., 2009b) and then converted to spectral irradiance (μW cm^{-2} nm^{-1}). Assuming the targets are uniform diffusers, the spectral irradiance value of the target was divided by the corresponding solar spectral irradiance to derive the RF.

Prior to sampling values from the target areas, daily-averaged reflectance factor (DARF) values were calculated from RF images taken at 10-min intervals from 0900 to 1500 JST each day. The advantage of using DARF instead of instantaneous RF values has been discussed in Shibayama et al. (2011a). We selected NIR images taken at three exposure speeds, 10, 20 and 30 (dimensionless), and at corresponding minimum threshold solar spectral irradiance levels, 30, 25 and 20 μW cm^{-2} nm^{-1}, selected according to Shibayama et al. (2011a). In the same manner, we selected RED images taken at exposure speeds of 0, 10 and 20, and at corresponding minimum threshold solar spectral irradiance levels, 70, 40 and 20 μW cm^{-2} nm^{-1}. Images taken at < 20 μW cm^{-2} nm^{-1} were omitted from daily averages. DARF images were obtained by averaging pixel-by-pixel for those whole images taken on each day fulfilling the above-mentioned conditions. Using DARF-RED and -NIR images, daily-averaged normalized difference vegetation index (DA-NDVI) images were provided by dividing the difference between DARF-NIR and DARF-RED with their sum pixel-by-pixel. Both band images were shifted horizontally ±9 pixels relative to each other to adjust the parallax observed at the central part of the images. Slightly mismatched pixels in the peripheral region were neglected.

From the viewing field of the cameras, 10 plots were targeted in the 2009 and 12 plots in the 2010 images (see Fig. 1). In DARF or DA-NDVI images, five horizontal lines from about 100 to 200 pixels were determined manually in each plot (Fig. 2, L2). The fixed coordinates of both sides of each line were used to take radiometric values in images throughout the entire cropping seasons.

4. Viewing geometry and equation of linear regression models

View direction angles for the target areas were defined on a two-dimensional diagram of the experimental paddy field. View angles (º) were: angle A, between a line from the PDC to the center of the target area and the planting row running through the target area; and angle B, between a line from the PDC to the target area and the meridian (Fig. 3). Both angles were derived from horizontally projected geometry excluding the vertical angular configuration, and only a single angle was represented for each plot in each year. In a previous study, we found no

effect of view zenith angle on DARF values (Shibayama et al. 2011b). Hence, the view direction angles A and B have been simply defined in a two-dimensional plane (Fig. 3). In this study, solar zenith angle (SZ, °) at the culmination on each day, the daily solar radiation (SR, MJ m^{-2}) and the duration of sunshine (DS, h) measured by the Weather Data Acquisition System of the National Institute for Agro-Environmental Sciences have been introduced as explanatory variables. The linear regression model equation is:

$$f(SPAD) = b_0 + b_1 X + b_2 \cos A + b_3 \cos B + b_4 \cos SZ + b_5 SR + b_6 DS. \quad (1)$$

Where, X is the radiometric variable derived from the PDC observation, which is described in the following section. f(SPAD) indicates transformations for SPAD such as logarithm and square in addition to the original SPAD value. Interaction terms between explanatory variables were also tested where appropriate. The performance of the model and each explanatory variable was evaluated using coefficient of determination (R^2), root-mean-square error (RMSE) and Student's t-value. JMP 7 software (SAS Institute Inc., Cary, NC, USA) was used for statistical analyses.

5. Leaf greenness index, mean1, mean2 and mean2/1

As radiometric variables to estimate SPAD values of rice leaves, we tested DARF-NIR, DA-NDVI and leaf greenness index (LGI). Using DARF-RED and DARF-NIR, DA-NDVI is defined as:

$$\text{DA-NDVI} = (\text{DARF-NIR} - \text{DARF-RED}) / (\text{DARF-NIR} + \text{DARF-RED}). \quad (2)$$

The dimensionless LGI tested in this study was derived by dividing DA-NDVI by DARF-NIR:

$$\text{LGI} = \text{DA-NDVI} / \text{DARF-NIR}. \quad (3)$$

The LGI is based on the idea that chlorophyll density per unit land area, corrected by the biomass per unit land area, could predict the chlorophyll content on a per plant or hill basis, which is roughly a measure of leaf greenness. Daughtry et al. (2000) demonstrated that combined use of two spectral vegetation indices was successful in producing isolines of leaf chlorophyll concentrations. Haboudane et al. (2002) introduced the use of the ratio of two different vegetation indices, TCARI and OSAVI*, to accurately predict corn leaf chlorophyll content from airborne remote sensing imagery. In estimates of chlorophyll content of corn leaves from hyperspectral images acquired by the Compact Airborne Spectrographic Imager, the new index ratio had a determination coefficient (R^2) of 0.804 with an RMSE of 4.35 μg cm^2. Tanaka et al. (2008), however, reported that TCARI/OSAVI was not outstandingly appropriate for estimating wheat chlorophyll content. Due to the limitation in available spectral bands, we employed a simpler index, LGI, obtained by dividing NDVI by RF-NIR. NDVI has been proven to detect the intercepted photosynthetically active radiation (PAR) in wheat (Hatfield et al., 1984) and rice (Leblon et al., 1991) and the absorbed PAR in corn canopies (Gallo et al., 1985). Intercepted or absorbed PAR should depend on the canopy chlorophyll density (Blackburn, 1998; Broge and Mortensen, 2002). On the other hand, RF-NIR has a close relationship to rice green biomass or leaf area per unit land area (Martin and Heilman, 1986; Shibayama and Akiyama, 1989). Our PDC has a calibration system to calculate RF to provide RF-NIR, which supplies the index LGI.

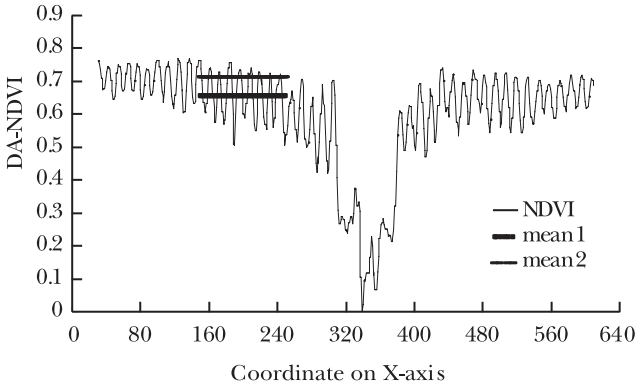

Fig. 4. Daily-averaged NDVI (DA-NDVI) values sampled on the line 'L1' in Fig. 2.
The short horizontal lines show two types of average values: mean1 and mean2.

Cross-sectional DA-NDVI in early-stage paddies (Fig. 2, L1) followed an odd-shaped curve (Fig. 4). Because NDVI responds to the green plant mass, pixels on the peaks may be on the plant rows and those in the troughs located on shaded plants or the soil and water surface. Due to insufficient spatial resolution of the cameras, it is impossible to identify each leaf of a plant. Therefore, we tested two averaging methods to obtain representative values of DA-NDVI and DARF-NIR for each plot. The first is simply averaging the whole pixel values on a sample line and then obtaining the baseline mean value for the five lines. This value is called 'mean1' in this article. The second method involves averaging only the radiometric values equal to the mean1 or above, and this derived value is called 'mean2' hereafter. Calculating mean2 was possible

*TCARI, transformed chlorophyll absorption in reflectance index: $=3[(R700-R670)-0.2\,(R700-R550)(R700/R670)]$; OSAVI, optimized soil-adjusted vegetation index: $=(1+0.16)(R800-R670)/(R800+R670+0.16)$ (Rondeaux et al., 1996).

only for image data but never for one-dimensional data from a unified field-of-view radiometer. We expected that mean2 would reduce the effects of shaded plants, soil, and water surface. Hence, LGI has three variants:

$$\text{LGImean1} = \text{DA-NDVImean1}/\text{DARF-NIRmean1}, \quad (4)$$

$$\text{LGImean2} = \text{DA-NDVImean2}/\text{DARF-NIRmean2}, \quad (5)$$

and

$$\text{LGImean2/1} = \text{DA-NDVImean2}/\text{DARF-NIRmean1}. \quad (6)$$

Results

1. Measured SPAD values and plant nitrogen content in paddy rice plots

Average 2010 SPAD values measured for each treatment (variety×topdressing) were relatively large (around 40) right after transplanting and started declining between 2 and 9 July (leaf number index: 9.8–10.2) to low values of 25–32 at the panicle formation stage (Fig. 5). The SPAD increased slowly after topdressing but declined again after heading. The standard deviation of the three measured SPAD values in each plot varied from 0.78 to 1.58 during the 2010 experiment. The seasonal variation of SPAD was largely common among the varieties and fertilizer levels. As shown in the 2009 data (Fig. 6), SPAD values for upper leaves were closely related to the plant nitrogen content, which varied from 7.53 to 38.75 g kg^{-1} (dry weight basis per hill). The coefficient of determination (R^2) was favorable at 0.799 and the relation seemed to be linear, which indicates that leaf color measured as SPAD could be converted to a measure of the total nitrogen level per plant hill in the middle to high nitrogen content ranges. Larger variations at the lower nitrogen content range might be due to nitrogen contents being measured for the whole plant, including stems and lower leaves, whereas the SPAD values were read on only the upper leaves.

2. Seasonal DARF, DA-NDVI and LGI observed for paddy rice

The 2010 seasonal patterns of DARF-RED, DARF-NIR and DA-NDVI were generally smooth curves (Fig. 7), although some spiking data points indicated there were several days of insufficient or rapidly fluctuating solar irradiance that did not allow stable DARF images to be acquired. Fortunately, we found no outliers in the matched-pair data of SPAD and PDC images used for the later analyses.

The DARF-NIR values increased steeply in the early vegetative growth period, and the rate of increment was reduced but linearly increased through heading until the middle maturing period, and then declined. The DARF-RED variation was downwardly convex, with the bottom point occurring just before the heading. The measured SPAD values apparently increased after the second

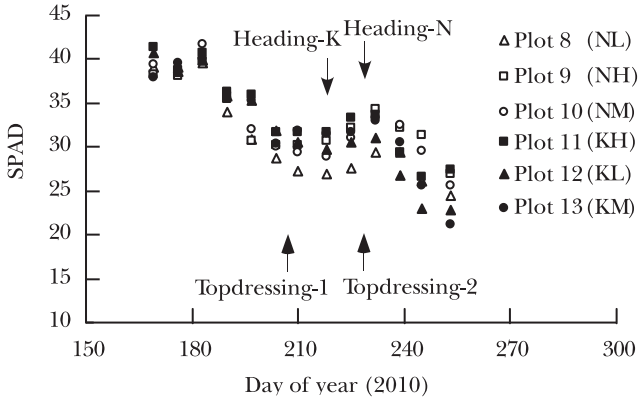

Fig. 5. Seasonal changes in measured SPAD values for the central plots (plots 8 through 13; see Fig. 1) in 2010. The two letters in parentheses indicate the rice varieties and fertilizer levels (see Fig. 1). Headings -K and -N indicate the heading dates observed for the varieties 'Koshihikari' and 'Nipponbare', respectively. Topdressing-1 indicates topdressings for the plots of fertilizer levels 'H' and 'M' at the late spikelet initiation stage, and topdressing-2 at the full heading stage for the 'H' plots. The growth stages were measured for 'Koshihikari'.

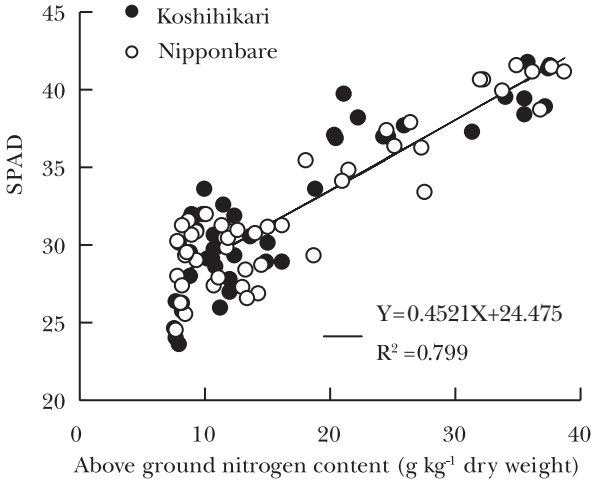

Fig. 6. Comparison of rice leaf SPAD values with above-ground plant nitrogen content (g kg^{-1}, dry weight basis) for two japonica varieties in 2009.

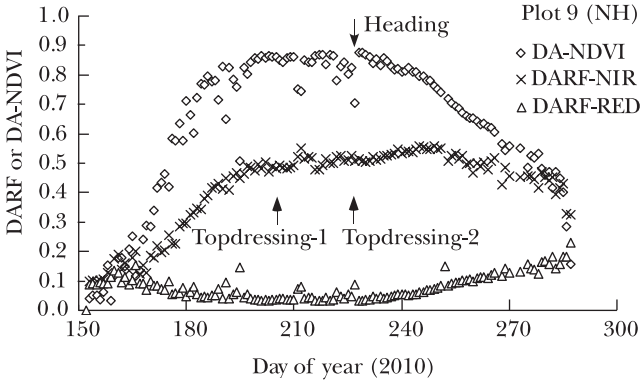

Fig. 7. Seasonal variation in DA-NDVI, DARF-NIR and DARF-RED observed in the 2010 trial for paddy rice plot 9 of variety 'Nipponbare' with total topdressing of 3 g N m^{-2}.

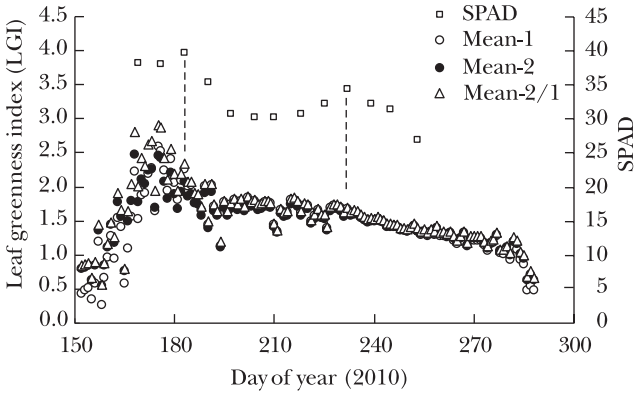

Fig. 8. Seasonal variation in leaf greenness index (LGI) and SPAD values observed for the paddy rice plot 9 in 2010. Three mean values are shown for LGI. The dashed lines indicate the observed peaks in SPAD values.

topdressing (Fig. 5), which would reduce RF in RED due to the increased chlorophyll absorption. However, the DARF-RED showed no further decrease (Fig. 7). The emerging panicles may influence the incident and/or reflected light in addition to the extremely strong absorption that already existed in the band. The DA-NDVI values increased more rapidly than DARF-NIR in the vegetative growing stages and reached a plateau at the same time as or slightly earlier than the turning point of DARF-NIR. The DA-NDVI kept the maximum value until heading, followed by a rapid decrease. Although NDVI is an index derived from RED and NIR (Eq. (2)), the three seasonal changing patterns differed. The averaging procedure used was 'mean1', which is a simple arithmetic mean for the variables shown in Fig. 7. Mean2 values differed slightly in the early growth period, when the plant incompletely covered the soil. However, seasonal patterns of mean1 and mean2 for each variable were basically the same. There was no obvious difference between averaging procedures in seasonal patterns throughout the cropping season that was detectable by eye (data not shown). The seasonal patterns, however, for DARF-RED, DARF-NIR and DA-NDVI differed obviously from the pattern for SPAD (Fig. 5).

Fig. 8 shows the representative seasonal patterns of LGI and SPAD. Except for the very early days after transplanting, when no SPAD survey had yet started due to the small size of the leaves, the changing directions and turning points of LGI roughly agreed with that of the SPAD. LGImean2/1 values were larger than LGImean1 and LGImean2 values in the early growth period. After heading, there were no obvious differences between LGImean1 and mean2 values, and LGImean2/1 values were slightly larger than the other two. Observing the seasonal variation of the tested variables, LGI seemed to be most closely related with the SPAD.

3. Correlations between SPAD and radiometric variables

DA-NDVI, DARF-NIR and LGI with three averaging procedures, mean1, mean2 and mean2/1, were regressed to the values of SPAD, $SAPD^2$ and $\log_e$ SPAD, and the results presented as R^2 values (Table 2). The R^2 values for DA-NDVI were lower than DARF-NIR and LGI. LGI had better R^2 values than DARF-NIR, with one exception. When the averaging methods were compared, mean2/1 was slightly better than the others, and the best R^2 value of 0.532 for 156 observations was obtained between $SPAD^2$ and LGImean2/1. The transformation $\log_e$ SPAD was not effective. The results were used for reference in the following stage of analysis.

4. Selection and performance of regression models for estimating paddy rice SPAD using digital images

Based on the correlation analyses, we tested several combinations of dependent and independent (explanatory) variables and their transformations. The top of Table 3 shows a representative regression analysis for the 2010 dataset, indicating that LGImean2/1 was a far more effective radiometric variable than DARF-NIR or DA-NDVI when the probability level (P) was the criterion. The variables cos B and cos SZ were statistically significant ($P<0.05$), although cos A was not significant. The bottom two tables are of each-year analysis using only LGImean2/1,

Table 2. Coefficients of determination (R^2) resulting from simple linear regression analysis of the radiometric variables measured using the PDC and the rice leaf SPAD values with the transformations obtained in 2010.

	SPAD			$SPAD^2$			$\log_e$ SPAD		
	mean1	mean2	mean2/1	mean1	mean2	mean2/1	mean1	mean2	mean2/1
DA-NDVI	0.156	0.161		0.194	0.199		0.117	0.122	
DARF-NIR	0.470	0.460		0.510	0.497		0.421	0.414	
LGI	0.476	0.502	0.506	0.492	0.523	0.532	0.452	0.474	0.471

DARF-NIR, daily-averaged reflectance factor in the NIR (820–900 nm) band; DA-NDVI, daily-averaged NDVI; LGImean2/1 indicates that DA-NDVImean2 was divided by DARF-NIRmean1 in the LGI calculation.

mean1, arithmetic mean of the pixel means of the values on the 5 horizontal lines in the plot.

mean2, arithmetic mean of the pixel means of the values that are equal to or greater than mean1 on the 5 horizontal lines in plot.

Table 3. Summary of multiple linear regression for estimating SPAD of paddy rice leaves using radiometric variables and geometrical parameters. Evaluation for all explanatory variables (upper table) and regression summaries for the selected three variables in the 2009 (middle table) and 2010 (bottom table) datasets. The dependent variable is $SPAD^2$.

Dependent variable: $SPAD^2$		R^2: 0.712, RMSE: 174.7, n: 156,		Year: 2010
Explanatory variable	Partial regression coefficient	Standard error	t	P
Intercept	−2696.8	677.4	−3.98	0.0001
LGImean2/1	256.0	62.6	4.09	<0.0001
DARF-NIRmean1	−351.6	435.6	−0.81	0.421
DA-NDVImean2	−380.6	293.2	−1.30	0.196
cos A	276.9	324.9	0.85	0.395
cos B	185.0	89.4	2.07	0.040
cos SZ	3584.5	621.6	5.77	<0.0001
Dependent variable: $SPAD^2$		R^2: 0.671, RMSE: 184.6, n: 156,		Year: 2010
Explanatory variable	Partial regression coefficient	Standard error	t	P
Intercept	−2922.9	401.2	−7.28	<0.0001
LGImean2/1	402.0	44.6	9.02	<0.0001
cos B	186.6	79.3	2.35	0.020
cos SZ	3355.2	476.2	7.05	<0.0001
Dependent variable: $SPAD^2$		R^2: 0.763, RMSE: 181.3, n: 140,		Year: 2009
Explanatory variable	Partial regression coefficient	Standard error	t	P
Intercept	−5166.0	318.9	−16.20	<0.0001
LGImean2/1	488.9	59.5	8.22	<0.0001
cos B	225.9	111.7	2.02	0.045
cos SZ	5564.6	345.2	16.12	<0.0001

A, angle (°) between a line from the camera to the center of the target area and the planting row running through that target; B, angle (°) between a line from the camera to the target area and the meridian; SZ, solar zenith angle (°) at the culmination; t, Student's t-value.

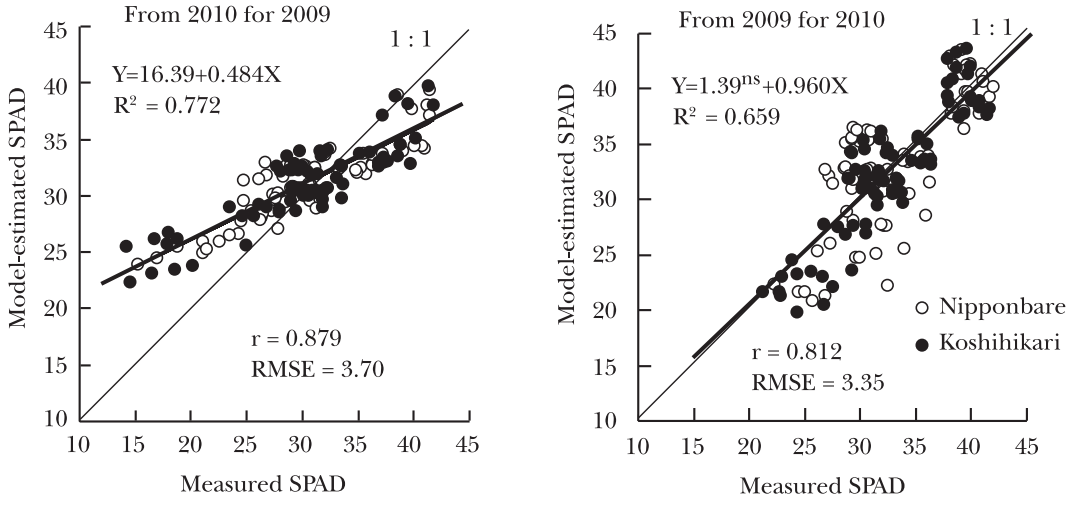

Fig. 9. Mutual predictions for rice leaf SPAD values obtained using digital images and Model 1 (Table 4) plotted against the measured SPAD values. Model parameters were derived from the 2010 dataset and the model was applied to the 2009 dataset (left). The performance in the inverse operation is shown in the scatter diagram on the right.

Table 4. Multiple regression models 1 to 5 for estimating paddy rice SPAD using LGI and observed geometric and weather condition data.

Model ID	Dependent variable	Explanatory variable							R^2
1	$SPAD^2$	LGImean2/1***	cos B*	cos SZ***					0.708
2	$SPAD^2$	LGImean2/1***	cos B***	cos SZ***	SR^{ns}	DS^{ns}	DS×cos SZ^{ns}	SR×cos SZ**	0.813
3	$SPAD^2$	LGImean2/1***	cos B***	cos SZ***	SR***			SR×cos SZ***	0.811
4	SPAD	LGImean2/1***	cos B***	cos SZ***	SR***			SR×cos SZ***	0.815
5	SPAD	$\log_e$ LGImean2/1***	$\log_e$ cos B***	$\log_e$ cos SZ***	$\log_e$ SR***			$\log_e$ SR×$\log_e$ SZ***	0.820

B, angle (°) between a line from the camera to the target area and the meridian; SZ, solar zenith angle (°) at the culmination; SR, daily solar radiation (MJ m^{-2}); $\log_e$ X, natural logarithm of X.
*, **, *** and ns respectively indicate significance at the 0.05, 0.01, and 0.001 level and no significance.

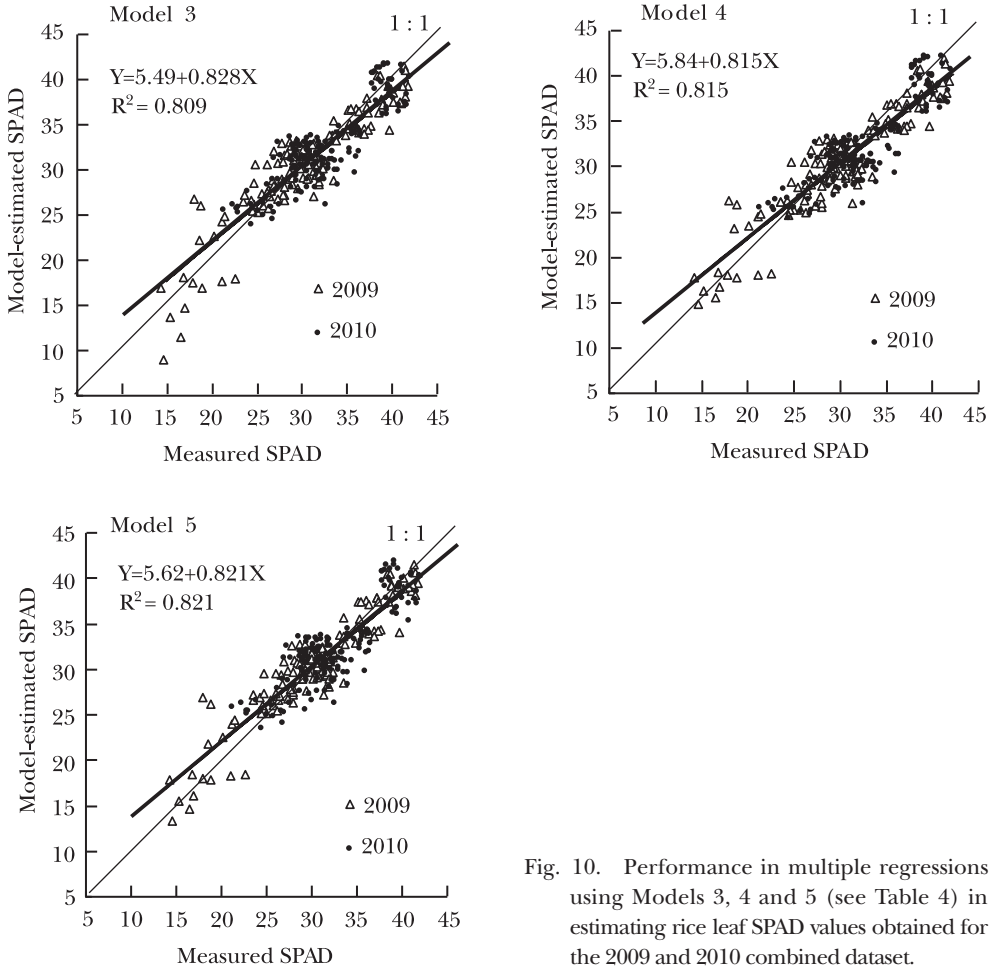

Fig. 10. Performance in multiple regressions using Models 3, 4 and 5 (see Table 4) in estimating rice leaf SPAD values obtained for the 2009 and 2010 combined dataset.

cos B and cos SZ, which were all statistically significant ($P<0.05$). The model derived from each year's dataset estimates $SPAD^2$ of another year, and its square-root values were plotted against the measured SPAD (Fig. 9). The model equation of 2009 estimated 2010 SPAD with a simple correlation coefficient (r) of 0.812 and an RMSE of 3.35, and the fitting between estimated and measured values was fair across the whole range. On the other hand, the 2009 SPAD values estimated by the 2010 model were linear with the measured value ($r=0.879$, RMSE=3.70), but a clear divergence from the line was observed in the lower and higher SPAD regions. No varietal difference was notified in the scattering diagrams.

To solve the problem of year-to-year applicability of model equations, we tested several regression equations using the two-year combined dataset (Table 4). The original equation (Model 1) was replenished with new variables: daily solar radiation (SR), duration of sunshine (DS), and their interaction terms with the original variables (Model 2). The variables SR and DS were

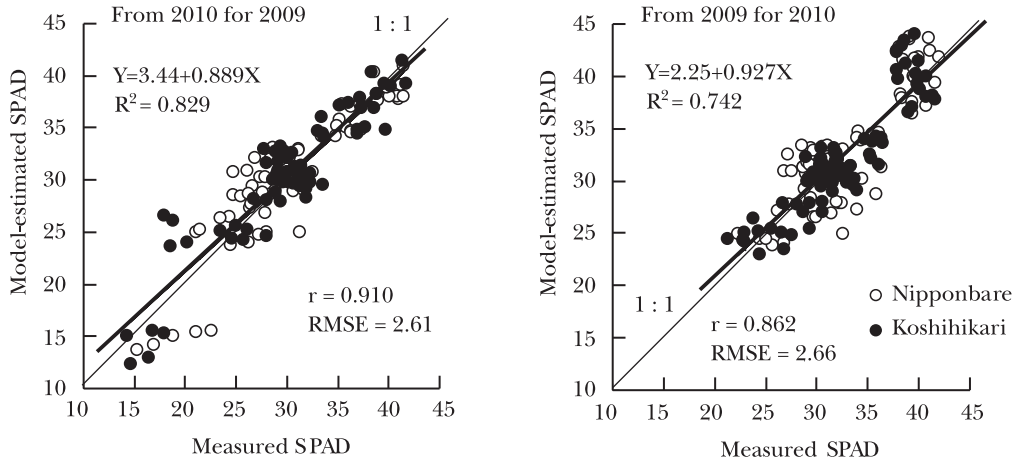

Fig. 11. Biennial mutual predictions for rice leaf SPAD values obtained using digital images and Model 4 (Table 4) plotted against the measured SPAD values from the 2010 dataset for the 2009 data (left) and from the 2009 dataset for the 2010 data (right).

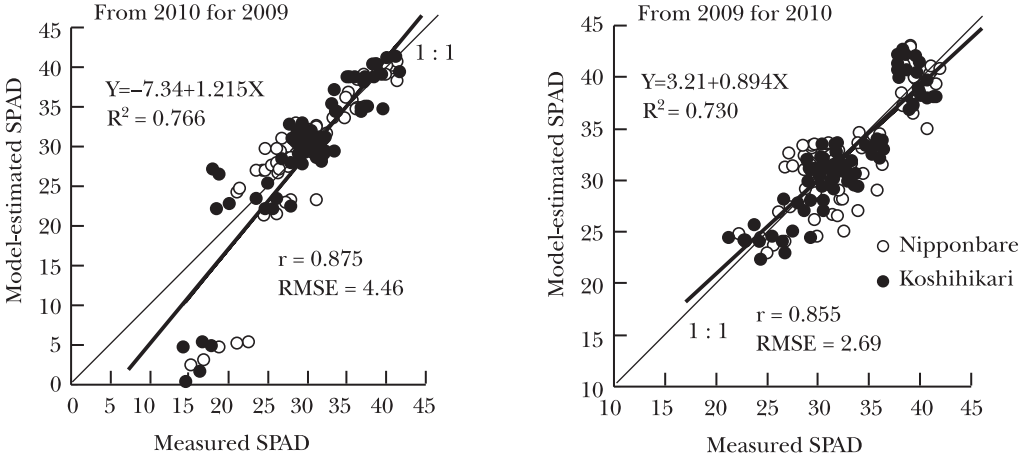

Fig. 12. Biennial mutual predictions for rice leaf SPAD values obtained using digital images and Model 5 (Table 4) plotted against the measured SPAD values from the 2010 dataset for the 2009 data (left) and from the 2009 dataset for the 2010 data (right).

introduced to reduce the year-to-year variation because we thought that weather conditions might have affected the calculated radiometric variables through an unknown mechanism. Analysis indicated that DS was not significant, but SR and the interaction term between SR and cos SZ were highly significant in the model (Model 3). However, measured and estimated SPAD values on the scattering diagram showed that the relationship was not necessarily linear across the whole SPAD range (Fig. 10). Then, replacing the dependent variables from $SPAD^2$ to SPAD, we obtained Model 4, then Model 5 by applying a natural logarithm transformation for the explanatory variables (Table 4). The coefficient of determination (R^2) for Model 4 was slightly larger (0.815) than that of Model 3 (0.811), and the largest R^2 value of 0.820 was achieved in Model 5.

Scattering diagrams of estimated versus measured SPAD for both Models 4 and 5 were close to a linear relationship, even though the slopes in the linear regression equations were less than 1.0 and the intercepts were significant (Fig. 10). We compared the year-to-year fitting performance of Models 4 and 5 to find that Model 4 gave a better result in the validation test (Fig. 11). Each model had the same common independent variables, but the partial regression coefficients were calculated using only a single-year dataset and applied to the other year's data. Model 4-estimated and measured SPAD values closely correlated, with r=0.910 and 0.862 and RMSE=2.61 and 2.66 in 2009 and 2010, respectively. However, Model 5, derived from the 2010 dataset, predicted extremely low SPAD values for 2009 (Fig. 12). At this stage of the study, we considered that Model 4 might be the best choice as the SPAD prediction model equation:

Table 5. Regression model for estimating paddy rice SPAD using LGI, view direction and solar direction, and weather station data of the 2009 and 2010 combined dataset.

Dependent variable: SPAD,	R^2: 0.815, RMSE: 2.46, n: 296			year: 2009+2010
Explanatory variable	Partial regression coefficient	Standard error	t	P
Intercept	−44.83	3.50	−12.99	<0.0001
LGImean2/1	7.85	0.49	16.00	<0.0001
cos B	3.68	0.87	4.24	<0.0001
cos SZ	65.97	4.05	16.28	<0.0001
SR	−0.09	0.03	−3.49	0.001
SR×cos SZ	−7.08	0.59	−11.93	<0.0001

B, angle (°) between a line from the camera to the target area and the meridian; SZ, solar zenith angle (°) at the culmination; SR, daily solar radiation (MJ m^{-2}); t, Student's t-value.
(SR−16.0)×(cos SZ−0.94).

$$SPAD = b_0 + b_1\ LGImean2/1 + b_2\ SR + b_3 \cos B + b_4 \cos SZ + b_5\ SR \times \cos SZ. \quad (7)$$

Table 5 presents the regression summary of Model 4 derived using the two-year combined dataset. Daily-predicted SPAD values were plotted against the day of year in 2010 as well as the measured SPAD values for the central two plots in the field of view (Fig. 13). The seasonal changing patterns of predicted and measured SPAD were roughly coincident; the digital images could predict the rapid decline in leaf greenness before the panicle formation stage. However, the differences in predicted values between the compared plots were not sufficiently obvious.

For the 2009 data, the aboveground nitrogen contents per plant hill were plotted against the predicted SPAD values using Model 4 (Fig. 14). We tested a cubic curve fit to the relationship and obtained an R^2 value of 0.950. The smooth-fitting curve with a relatively small variation indicates that the spectral digital imaging technique offers the possibility to directly predict plant nitrogen content throughout the rice cropping season.

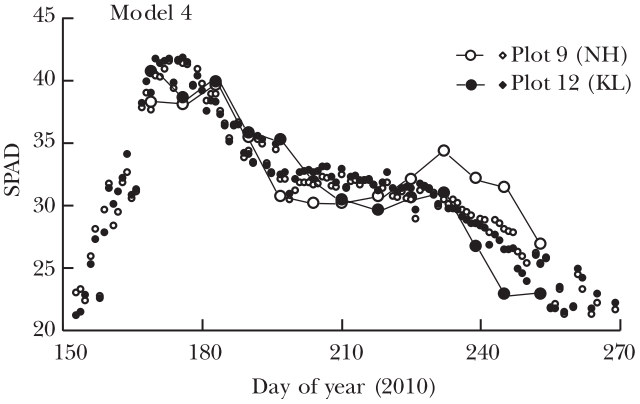

Fig. 13. Seasonal variations of measured SPAD values (large circles) and model-estimated values (Model 4, small circles) for the central two plots in 2010.

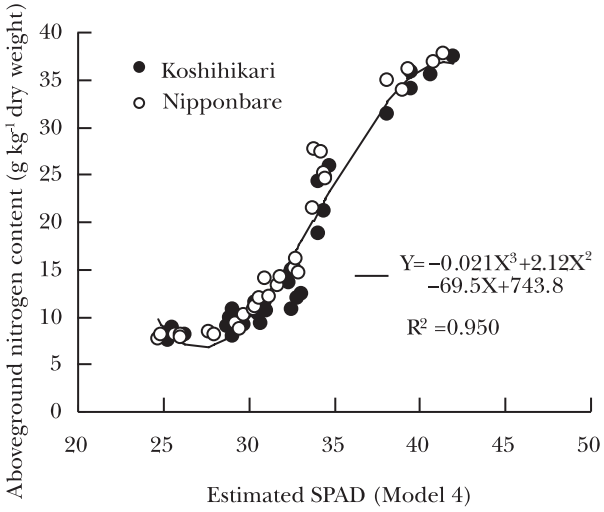

Fig. 14. Comparison of estimated SPAD values obtained from digital images using Model 4 with the aboveground nitrogen content of paddy rice plant hills measured in 2009.

Discussion

1. Measured SPAD values

The response of SPAD values to leaf chlorophyll and/or nitrogen content has been evaluated for various crops (Monje and Bugbee, 1992; Minotti et al., 1994; Shimada et al., 1995; Johnkutty and Palaniappan, 1996; Chapman and Barreto, 1997; Bullock and Anderson, 1998; Yasumoto et al., 2011) and rice varieties (Huang et al., 2008). SPAD values vary depending on the measured position on the leaf blade as well as the leaf position on the stem (Lin et al., 2010). Other studies have reported effects on SPAD values from specific leaf weight (Peng et al., 1993; 1995), solar irradiance (Hoel and Solhaug, 1998) and equipment type (Monje and Bugbee, 1992). In the present study,

however, a priority was the traceability of seasonal changes in greenness. At this stage of our development of a technique to detect leaf color change of a single crop species (two major paddy rice varieties growing in Japan), direct use of SPAD values without conversion to actual chlorophyll or nitrogen content may be acceptable, although excessive generalization of the result obtained from this small-scale experiment should be avoided. We paid attention to uniformity in plant growth in each plot. The requirement for representativeness of the SPAD measured in each plot might be satisfied, since the standard deviation of three measured SPAD values in each plot was no more than 5% of the mean SPAD value during the 2010 experiment.

2. Evaluation of LGI

The seasonal trend in LGI was different from that of either DA-NDVI or DARF-NIR, which were used to derive LGI. By visual observation, seasonal patterns of LGI agreed well with that of leaf greenness measured with SPAD. The seasonal changes in SPAD are rather complicated, depending on plant growth stage as well as fertilizer application and environmental factors (Turner and Jund, 1994; Huang et al., 2008). The SPAD values remained large in the early vegetative growth stages and declined rapidly until the panicle formation stage, when topdressing was applied. The values slowly increased to the mid-maturity, then again decreased swiftly. The RF-RED, RF-NIR and NDVI could not follow the seasonal trend in SPAD values, probably because SPAD indicates chlorophyll content per unit leaf area instead of total chlorophyll amount per unit land area, or the field of view of the sensor.

Matsuda et al. (2003) succeeded in evaluating leaf greenness and nitrogen content of crop plants using a commercial digital camera capturing red, green and blue color images. Okada and Ikeba (2008) reported that NDVI images taken with a specialized digital camera were effective for assessing leaf greenness of paddy rice. These techniques have proven effective to evaluate leaf color differences within an image acquired at a particular moment, and should be usable in some practical applications. However, seasonal patterns of those indices have not been widely tested. On the other hand, as shown in Fig. 13, the LGI less effectively detected the difference in SPAD values among the plots of varieties and/or fertilizer levels on a single observation date even though the order in SPAD levels between plots was almost correctly estimated. It is supposed that daily-averaging for RF might obscure the differences in LGI among the plots in the viewing field. The previously referred studies (Matsuda et al., 2003; Okada and Ikeba, 2008) though, have already proved the capability of digital camera images for evaluating variations in rice leaf greenness in each image. Further investigations are needed to examine the LGI derived at a moment instead of daily-averaged for the detection capability among plots. We may have to reserve judgment but future works will indicate some modifications in the model such as introducing growth-stage-dependent parameters, or combined use of different radiometric indices that respectively correspond to the seasonal and plot-to-plot differentiation. The LGI requires an NIR channel as well as RED to provide NDVI using solar irradiance sensing to derive an RF for NIR, which indicates that a commercial digital camera in situ is not usable for LGI. However, LGI requires only two narrow-band channels that can be detected by simple equipment, such as a modified digital camera equipped with low-cost filters. Further work from various viewpoints is needed to confirm these results.

3. LGI means of cross-sectional lines in images with medium spatial resolution

The spatial resolution of the cameras in PDC was not sufficient to observe each leaf blade from the employed camera position. Hence, we used averaged radiometric variables sampled on five horizontal lines that cross the planting rows and were arbitrarily decided for each plot based on the assumption that the values obtained may not differ much from the area-averaged values. Future studies using higher spatial resolution cameras could evaluate the spatial distribution of greenness in the field and in each plot and row or hill. Further close-range imaging may reveal color divergence in a plant or organ (Shibayama et al., 2009a), but it could not be acquired at the same time with measurement at the field level or higher.

To estimate SPAD values of leaves, isolation of sunlit green leaves from background, such as shaded plant parts and soil and water surfaces, may be essential. While our LGI aims to detect solely leaf color instead of the total amount of pigment per unit land area, a simple average of LGI in an area would be inadequate, because it includes every part of various targets in the target area, and this distorts the calculated values. The discrepancy may be reduced after the plant covers 100% of the land, and that timepoint comes earlier when adopting shallow camera angles. For images of insufficient spatial resolution, we used two calculation methods to derive mean values on a sample line perpendicularly crossing the planting rows: the first is the simple arithmetic mean (mean1), and the second is the mean of values equal to and above the mean1 (mean2). The mean2 was introduced due to its simplicity. The effect of mean2 was not very drastic, but it proved effective to some extent in the correlation analyses. It should be noted that the LGImean2/1 value was better than LGImean1 or LGImean2. This combination seems reasonable because DA-NDVImean2 indicates photosynthetic activity only in relatively dense plant areas,

and DARF-NIRmean1 responds to the total biomass per unit land area. Therefore, LGImean2/1 is a more theoretically appropriate index to evaluate leaf greenness with less influence of biomass, leaf area and background. The tested calculation utilizes characteristics of image data, and furthermore, improved estimation accuracy under the given conditions of camera spatial resolution, crop species and cultivation practice. However, further refinement and testing are necessary. For instance, it is unknown whether the technique would be effective for images acquired at other spatial resolutions, images of broadcast sown crops, or for different planting row orientations from those employed in this experiment. For images with finer spatial resolution, repeated application of the procedure to calculate mean2 may extract radiometric values that solely come from the upper sunlit part of the crop canopy.

4. Equations and parameters of LGI models for predicting SPAD

We described our heuristic procedure for deriving multiple regression models to estimate SPAD using LGImean2/1. The dependent variable was $SPAD^2$ in the early stages, judging by the results of simple correlation analyses. Later, we returned to SPAD because of better linearity between measured and estimated values in the models used. Model 5, which has logarithmic transformations of all explanatory variables, showed the best performance on the basis of R^2 value. The model assumes that the effect of each explanatory variable can be expressed as a property of multiplication. This seemed to be more reasonable than the additive models, Models 1 through 4, as a general model of radiometric evaluation for illuminated leaf color. In this study, however, we tentatively adopted additive Model 4 as the final form of the equation because of its better biennial applicability. We have not probed the cause of variance in Model 5.

View angles A and B were introduced in previous studies predicting LAI of paddy rice using a PDC (Shibayama et al., 2011a, 2011b). Regression analyses for SPAD prediction, however, rejected the term cos A, although cos B has been employed even in the latest model. View angle A is defined between the view direction and planting row, and view angle B is between the view and meridian directions. The term of angle A may correct for the shading effect on the plant rows and might be reduced by the mean2 calculations. On the other hand, angle B is related to the view and solar directions. Although DARF and DA-NDVI are daily-averaged values, the angle between view and sun position at the culmination of each day plays an important role in the model equation. Even after the daily averaging, bidirectional characteristics of the plant canopy on radiometric variables remained influential. We speculate that cos B is a simple but effective parameter that could reduce the effect from bidirectional reflectance distribution. The daily highest solar zenith angle at the culmination on each day (SZ), also proved an effective parameter in this study. The term cos SZ may play a complementary role with cos B to reduce the bidirectional reflectance characteristics. Multiple sun-angle data acquisition was recommended to extract information for erectophile canopies like wheat (Pinter, Jr. et al., 1985). Daily-averaging for RF in each band should reduce the influence on LGI of paddy rice, which also has an erectophile canopy. However, there remained an uncorrected fraction of the total deviation in LGI due to the SZ. How the two fixed parameters could correct daily-averaged radiometric variables is unknown, because B is a constant for a targeted point, and SZ is only a single value defined each day.

To reduce the biennial differences in applicability of the original model, we introduced the parameters SR and DS. We found that DS was ineffective but SR and the interaction term between SR and cos SZ were statistically significant in the models. SR was used to correct for differences in incident illumination conditions in the two seasons because the remaining parameters, cos B and cos SZ, are fixed between the two years. SR represents the weather conditions of the day: cloud cover and cloud thickness. A PDC has solar irradiance sensors to calculate RF, and a daily averaging procedure for DARF is expected to reduce the random error and deviation caused by the weather and view and illumination angles (Shibayama et al., 2009b). However, two additional parameters indicate that leaf color assessment requires additional correction of radiometric variables, compared to estimation of nitrogen uptake (Shibayama et al., 2009b) or LAI (Shibayama et al. 2011a, 2011b). The significant interaction term of SR and cos SZ suggests that instantaneous use of SZ at the time of collection of each image and calculation of RF would improve prediction accuracy and reliability. However, further considerations will be required to develop an appropriate algorithm to modify the PDC system. The practical advantage of SR and SZ is that they can be conveniently obtained from a local weather station and simple calculations.

5. Direct use of LGI to predict nitrogen content

A close relationship between estimated SPAD values and nitrogen content of plant bodies supported development of automated diagnostic monitoring for crops using a digital image collection system. The relationship was nonlinear, but it showed less variation than the relationship between SPAD and nitrogen content (Figs. 6 and 14). The nitrogen content was obtained for the entire aboveground plant body but the SPAD was measured for the uppermost leaves. This could cause some errors in the relationship. However, the model-estimated SPAD values had a better performance than the original SPAD data. This result was

not expected beforehand and the causes are unknown but a feasible explanation may be that the LGI values were obtained not only from the uppermost leaves but also from other plant parts, including stems, panicles and lower leaves. Even though the procedure calculating mean2 for DA-NIDVI lessened the influence, the LGI values obtained did not exclusively arise from the upper leaves. In fact, it is more feasible to imagine that LGI reflects the whole sunlit plant, rather than only part when the restricted spatial resolution of cameras is considered. Although more studies employing images of finer spatial resolutions and a larger data set including nitrogen content are required, this aspect leads to that the model should directly estimate the nitrogen content of plant bodies instead of using SPAD as a mediational parameter.

The finding, however, shows that a PDC and digital image collection techniques could be useful to estimate seasonal nitrogen content and nitrogen uptake for a given land area simultaneously. Separate estimates of both values have been essential for accurately assessing characteristics of a specific crop variety in a given location in fluctuating weather conditions. Refinement of the techniques may contribute to improvement of field research, leading to better farm management through low-cost assessment of nitrogen.

Conclusions

Regression-based models predicted SPAD of rice leaves based on remotely obtained image data for canopy levels observed with low-cost digital cameras and solar sensors. Model parameters were daily-averaged reflectance factors in the DARF-RED and DARF-NIR, the angle between the view azimuth and the meridian directions, the solar zenith angle at the culmination and daily solar radiation. We introduced an LGI that is a ratio of daily-averaged NDVI divided by DARF-NIR, which followed the seasonal changes in SPAD well. Estimation accuracy was improved by a simple calculation utilizing the characteristics of image data to extract LGI measured principally from sunlit and dense plant parts.

Biennial trials of the regression models tested prediction accuracy over growing seasons, and model predications agreed well with SPAD values measured on the uppermost leaves. The estimated SPAD values from the LGI model showed a close relationship with the nitrogen content of plant body. Unmanned data collection and leaf greenness prediction will reduce plant disturbance, increase accuracy of data collection and reduce costs for experimental field surveys as well as chemical analysis.

Acknowledgments

Thanks are due to Hiroyuki Iino and Terushi Kamada at the National Institute for Agro-Environmental Sciences for their technical support in field experiments.

References

Abe, N., Fukuyama, T. and Kimura, H. 2007. Relationship between growth stages of rice and protein content in rice cultivar "Koshihikari" of earthquake damaged area. *Annual Report of Research Center for Natural Hazard and Disaster Recovery*, Niigata Univ., Niigata, Japan, 1: 137-141*.

Ahmad, I.S., Reid, J.F., Noguchi, N. and Hansen, A.C. 1999. Nitrogen sensing for precision agriculture using chlorophyll maps. *In*, ASAE Meeting Presentation. 18-21 July, 1999, Toronto, Canada, No. 993035: 1-14.

Akiyama, T. and Kawamura, K. 2003. Study of cloud cover ratio of Landsat-5 for the application on agriculture and forestry. *J. Jpn. Soc. Photogramm. Remote Sens.* 42(3): 29-34*.

Asaka, D. and Shiga, H. 2003. Estimating rice grain protein contents with SPOT/HRV data acquired at maturing stage. *J. Remote Sens. Soc. Jpn.* 23: 451-457*.

Asaka, D., Hayashi, T. and Shiga, H. 2006. The map for grain protein content of winter wheat using satellite observed NDVI at maturing stage. *J. Jpn. Agric. Systems Soc.* 22: 89-98*.

Balasubramanian, V. 1999. Farmer adoption of improved nitrogen management technologies in rice farming: technical constraints and opportunities for improvement. *Nutr. Cycl. Agroecosys.* 53: 93-101.

Blackburn, G.A. 1998. Quantifying chlorophylls and carotenoids at leaf and canopy scales: an evaluation of some hyperspectral approaches. *Remote Sens. Environ.* 66: 273-285.

Broge, N.H. and Mortensen, J.V. 2002. Deriving green crop area index and canopy chlorophyll density of winter wheat from spectral reflectance data. *Remote Sens. Environ.* 81: 45-57.

Bullock, D.G. and Anderson, D.S. 1998. Evaluation of the Minolta SPAD-502 chlorophyll meter for nitrogen management in corn. *J. Plant Nutr.* 21: 741-755.

Casadesus, J., Kaya, Y., Bort, J., Nachit, M.M., Araus, J.L., Amor, S., Ferrazzano, G., Maalouf, F., Maccaferri, M., Martos, V., Ouabbou, H. and Villegas, D. 2007. Using vegetation indices derived from conventional digital cameras as selection criteria for wheat breeding in water-limited environments. *Ann. Appl. Biol.* 150: 227-236.

Chapman, S.C. and Barreto, H.J. 1997. Using a chlorophyll meter to estimate specific leaf nitrogen of tropical maize during vegetative growth. *Agron. J.* 89: 557-562.

Daughtry, C.S.T., Walthall, C.L., Kim, M.S., Brown de Colstoun, E. and McMurtrey III, J.E. 2000. Estimating corn leaf chlorophyll concentration from leaf and canopy reflectance. *Remote Sens. Environ.* 74: 229-239.

Dobermann, A. 2003. Estimating indigenous nutrient supplies for site-specific nutrient management in irrigated rice. *Agron. J.* 95: 924-935.

Emori, Y. and Yasuda, Y. 1985. Optics in field spectrometry. *J. Jpn. Soc. Photogramm. Remote Sens.* 24(special issue I): 5-18***.

Esfahani, M., Abbasi, H.R.A., Rabiei, B. and Kavousi, M. 2008. Improvement of nitrogen management in rice paddy fields using chlorophyll meter (SPAD). *Paddy Water Environ.* 6: 181-188.

Gallo, K.P., Daughtry, C.S.T. and Bauer, M.E. 1985. Spectral estimation of absorbed photosynthetically active radiation in corn canopies. *Remote Sens. Environ.* 17: 221-232.

Haboudane, D., Miller, J.R., Tremblay, N., Zarco-Tejada, P.J., and Dextraze, L. 2002. Integrated narrow-band vegetation indices for prediction of crop chlorophyll content for application to precision agriculture. *Remote Sens. Environ.* 81: 416-426.

Hatfield, J.L., Asrar, G. and Kanemasu, E.T. 1984. Intercepted photosynthetically active radiation estimated by spectral reflectance. *Remote Sens. Environ.* 14: 65-75.

Hoel, B.O. and Solhaug, K.A. 1998. Effect of irradiance on chlorophyll estimation with the Minolta SPAD-502 leaf chlorophyll meter. *Ann. Bot.* 82: 389-392.

Huang, J., He, F., Cui, K., Buresh, R.J., Xu, B., Gong, W. and Peng, S. 2008. Determination of optimal nitrogen rate for rice varieties using a chlorophyll meter. *Field Crops Res.* 105: 70-80.

Inoue, Y. and Peñuelas, J. 2001. An AOTF-based hyperspectral imaging system for field use in ecophysiological and agricultural applications. *Int. J. Remote Sens.* 22: 3883-3888.

Jia, L., Chen, X., Zhang, F., Buerkert, A. and Römheld, V. 2004. Use of digital camera to assess nitrogen status of winter wheat in the Northern China Plain. *J. Plant Nutr.* 27: 441-450.

Johnkutty, I. and Palaniappan, S.P. 1996. Use of chlorophyll meter for nitrogen management in lowland rice. *Fert. Re.* 45: 21-24.

Kawashima, S. and Nakatani, M. 1998. An algorithm for estimating chlorophyll content in leaves using a video camera. *Ann. Bot.* 81: 49-54.

Ku, H.H., Kim, S.H., Choi, K.S., Eom, H-Y., Lee, S-E., Yun, S-G. and Kim, T.W. 2004. Nondestructive and rapid estimation of chlorophyll content in rye leaf using digital camera. *Korean J. Crop Sci.* 49: 41-45.

Leblon, B., Guerif, M. and Baret, F. 1991. The use of remotely sensed data in estimation of PAR use efficiency and biomass production of flooded rice. *Remote Sens. Environ.* 38: 147-158.

Lee, Y.J., Yang, C.M., Chang, K.W. and Shen, Y. 2011. Effects of nitrogen status on leaf anatomy, chlorophyll content and canopy reflectance of paddy rice. *Bot. Studies* 52: 295-303.

Lin, F.F., Qiu, L.F., Deng, J. S., Shi, Y.Y., Chen, L.S. and Wang, K. 2010. Investigation of SPAD meter-based indices for estimating rice nitrogen status. *Comput. Electron. Agric.* 71: 60-65.

Martin, R.D. Jr. and Heilman, J.L. 1986. Spectral reflectance patterns of flooded rice. *Photogramm. Eng. Remote Sens.* 52: 1885-1890.

Matsuda, M., Ozawa, S., Hosaka, Y., Kaneda, K. and Yamashita, H. 2003. Estimation of plant growth in paddy field based on proximal remote sensing–Measurement of leaf nitrogen contents by using digital camera. *J. Remote Sens. Soc. Jpn.* 23: 506-515*.

Matsushima, S., Matsuzaki, A. and Tomita, T. 1970. Analysis of yield-determining process and its application to yield-prediction and culture improvement of lowland rice. CI. On a method for expressing the leaf-colour of rice plants under field conditions (1). *Jpn. J. Crop Sci.* 39: 231-236*.

Matsushima, S. 1976. Cultural practices in the late growth period. *In*, High-Yielding Rice Cultivation. University of Tokyo Press, Tokyo, Japan. 311-353.

Minekawa, Y., Oda, K., Mori, S. and Kosugi, Y. 2007. Salt breezed damage analyses for rice paddy by reenact experiments. *J. Remote Sens. Soc. Jpn.* 27: 205-214*.

Minotti, P.L., Halseth, D.E. and Sieczka, J.B. 1994. Field chlorophyll measurements to assess the nitrogen status of potato varieties. *Hortscience* 29: 1497-1500.

Monje. O.A. and Bugbee, B. 1992. Inherent limitations of nondestructive chlorophyll meters: a comparison of two types of meters. *Hortscience* 27: 69-71.

Mori, S., Yokoyama, K. and Fujii, H. 2010. Classification of brown rice with different protein content using the diagnosis of leaf color during the ripening period in Shonai Area of Yamagata Prefecture. *Jpn. J. Crop Sci.* 79: 113-119*.

Nagano, T. and Shigedomi, O. 2005. The method of measuring leaf color by digital camera. *Kyushu Nogyo Kenkyu.* 67: 7**.

Nakatani, M. and Kawashima, S. 1994. An attempt to assess leaf color of winter cereals using a simple video system. *Jpn. J. Crop Sci.* 63: 42-47*.

Okada, S. and Ikeba, M. 2008. Study of the easy method for crop diagnosis by multi-spectral camera in a paddy field. *Proc. 44th Conf. Remote Sens. Soc. Jpn.* 171-172**.

Omine, M. 2007. Spectrum digital camera for growth sensing of soybeans. *J. Jpn. Soc. Agric. Machinery* 69: 18-20**.

Peng, S., Garcia, F.V., Laza, R.C. and Cassman, K.G. 1993. Adjustment for specific leaf weight improves chlorophyll meter's estimate of rice leaf nitrogen concentration. *Agron. J.* 85: 987-990.

Peng, S., Laza, R.C., Garcia, F.V. and Cassman, K.G. 1995. Chlorophyll meter estimates leaf area-based nitrogen concentration of rice. *Commun. Soil Sci. Plant Anal.* 26: 927-935.

Pinter, P.J. Jr., Jackson, R.D., Ezra, C.E. and Gausman, H.W. 1985. Sun-angle and canopy-architecture effects on the spectral reflectance of six wheat cultivars. *Int. J. Remote Sens.* 6: 1813-1825.

Rondeaux, G., Steven, M. and Baret, F. 1996. Optimization of soil-adjusted vegetation indices. *Remote Sens. Environ.* 55: 95-107.

Sakamoto, T., Shibayama, M., Takada, E., Inoue, A., Morita, K., Takahashi, W., Miura, S. and Kimura, A. 2010. Detecting seasonal changes in crop community structure using day and night digital images. *Photogramm. Eng. Remote Sens.* 76: 713-726.

Sen, A., Srivastava, V.K., Singh, M.K., Singh, R.K. and Kumar, S. 2011. Leaf color chart vis-a-vis nitrogen management in different rice genotypes. *Am. J. Plant Sci.* 2: 223-236.

Shibayama, M. and Akiyama, T. 1986a. A spectroradiometer for field use. VI. Radiometric estimation for chlorophyll index of rice canopy. *Jpn, J. Crop Sci.* 55: 433-438.

Shibayama, M. and Akiyama, T. 1986b. A spectroradiometer for field use. VII. Radiometric estimation of nitrogen levels in field rice canopies. *Jpn. J. Crop Sci.* 55: 439-445.

Shibayama, M. and Akiyama, T. 1989. Seasonal visible, near-infrared and mid-infrared spectra of rice canopies in relation to LAI and above-ground dry phytomass. *Remote Sens. Environ.* 27: 119-127.

Shibayama, M., Sakamoto, T., Homma, K., Okada, S. and Yamamoto, H. 2009a. Daytime and nighttime field spectral imagery of ripening paddy rice for determining leaf greenness and 1000-grain weight. *Plant Prod. Sci.* 12: 307-318.

Shibayama, M., Sakamoto, T., Takada, E., Inoue, A., Morita, K., Takahashi, W. and Kimura, A. 2009b. Continuous monitoring of visible and near-infrared band reflectance from a rice paddy for determining nitrogen uptake using digital cameras. *Plant Prod. Sci.* 12: 293-306.

Shibayama, M., Sakamoto, T., Takada, E., Inoue, A., Morita, K., Takahashi, W. and Kimura, A. 2011a. Estimating paddy rice leaf area index with fixed point continuous observation of near infrared reflectance using a calibrated digital camera. *Plant Prod.*

Sci. 14: 30-46.

Shibayama, M., Sakamoto, T., Takada, E., Inoue, A., Morita, K., Yamaguchi, T., Takahashi, W. and Kimura, A. 2011b. Regression-based models to predict rice leaf area index using biennial fixed point continuous observations of near infrared digital images. *Plant Prod. Sci.* 14: 365-376.

Shimada, S., Kokubun, M. and Matsui, S. 1995. Effects of water table on physiological traits and yield of soybean. I. Effect of water table and rainfall on leaf chlorophyll content, root growth and yield. *Jpn. J. Crop Sci.* 64: 294-303.

Spiertz, J.H.J. 2010. Nitrogen, sustainable agriculture and food security. A review. *Agron. Sustain. Dev.* 30: 43-55.

Suenobu, S., Kadoshige, K., Yamamoto, T. and Inoue, K. 1994. Nitrogen nutritional diagnosis of rice plant 'Hinohikari'. (2) Estimation of nitrogen absorption amount from plant height, number of tillers and leaf color. *Bull. Fukuoka Agric. Res. Cent.* A-13: 5-8*.

Takada, E., Inoue, A., Shibayama, M., Sakamoto, T., Morita, K., Kimura, A. and Takahashi, W. 2009. Growth condition estimation of rice by fixed point camera images. *J. Jpn. Agric. Systems Soc.* 25: 27-34*.

Takahashi, W., Vu, N.C., Kawaguchi, S., Minamiyama, M. and Ninomiya, S. 2000. Statistical models for prediction of dry weight and nitrogen accumulation based on visible and near-infrared hyper-spectral reflectance of rice canopies. *Plant Prod. Sci.* 3: 377-386.

Takebe, M. and Yoneyama, T. 1989. Measurement of leaf color scores and its implication to nitrogen nutrition of rice plants. *JARQ* 23: 86-93.

Takebe, M., Yoneyama, T., Inada, K. and Murakami, T. 1990. Spectral reflectance ratio of rice canopy for estimating crop nitorgen status. *Plant Soil* 122: 295-297.

Takemine, S., Rikimaru, A., Takahashi, K. and Higuchi, Y. 2007. Basic study for estimation of nitrogen content of rice plants from vegetation cover rate of rice obtained by a simple image measurement. *J. Jpn. Soc. Photogramm. Remote Sens.* 46(4): 61-65*.

Tanaka, S., Goto, S., Maki, M., Akiyama, T., Muramoto, Y. and Yoshida, K. 2008. Estimation and validation of leaf chlorophyll concentration in winter wheat at heading to anthesis stage using ground-based and aerial hyperspectral data. *J. Jpn. Soc. Photogramm. Remote Sens.* 47(2): 39-49*.

Turner, F.T. and Jund, M.F. 1994. Assessing the nitrogen requirements of rice crops with a chlorophyll meter. *Aust. J. Exp. Agric.* 34: 1001-1005.

Wada, G. 1969. The effects of nitrogen nutrition on the yield-determining process of rice plant. *Bull. Nat. Inst. Agr. Sci.* A-16: 27-167*.

White, M.A., Asner, G.P., Nemani, R.R., Privette, J.L. and Running, S.W. 2000. Measuring fractional cover and leaf area index in arid ecosystems: digital camera, radiation transmittance, and laser altimetry methods. *Remote Sens. Environ.* 74: 45-57.

Yasumoto, S., Suzuki, K., Matsuzaki, M., Hiradate, S., Oose, K., Hirokane, H. and Okada, K. 2011. Effects of plant residue, root exudate and juvenile plants of rapeseed (*Brassica napus* L.) on the germination, growth, yield, and quality of subsequent crops in successive and rotational cropping systems. *Plant Prod. Sci.* 14: 339-348.

Zhu, Y., Tian, Y., Yao, X., Liu, X. and Cao, W. 2007. Analysis of common canopy reflectance spectra for indicating leaf nitrogen concentrations in wheat and rice. *Plant Prod. Sci.* 10: 400-411.

* In Japanese with English summary.
** In Japanese with English title.
*** In Japanese.